CrossMark

ORIGINAL CONTRIBUTION

RLV-TD Flight Measured Aeroacoustic Levels and its Comparison with Predictions

K. Manokaran[1] · M. Prasath[1] · B. Venkata Subrahmanyam[1] · V. R. Ganesan[1] ·
Archana Ravindran[1] · C. Babu[1]

Abstract The Reusable Launch Vehicle-Technology Demonstrator (RLV-TD) is a wing body configuration successfully flight tested. One of the important flight measurements is the acoustic levels. There were five external microphones, mounted on the fuselage-forebody, wing, vertical tail, inter-stage (ITS) and core base shroud to measure the acoustic levels from lift-off to splash down. In the ascent phase, core base shroud recorded the overall maximum at both lift-off and transonic conditions. In-flight noise levels measured on the wing is second highest, followed by fuselage and vertical tail. Predictions for flight trajectory compare well at all locations except for vertical tail (4.5 dB). In the descent phase, maximum measured OASPL occurs at transonic condition for the wing, followed by vertical tail and fuselage. Predictions for flight trajectory compare well at all locations except for wing (− 6.0 dB). Spectrum comparison is good in the ascent phase compared to descent phase. Roll Reaction control system (RCS) thruster firing signature is seen in the acoustic measurements on the wing and vertical tail during lift-off.

Keywords Sound pressure level · Spectrum · Transonic · Flight measurements · RLV-TD

✉ K. Manokaran
manoo_krish@yahoo.co.in

[1] Aeronautics Entity, ADTG, Vikram Sarabhai Space Centre, Indian Space Research Organisation, Trivandrum, Kerala, India

Introduction

Reusable Launch Vehicle-Technology Demonstrator (RLV-TD) is a double delta wing body configuration placed over the top of solid booster with four fins mounted on the core base shroud to reduce the aerodynamic instability in the ascent phase. The fuselage forebody is blunt ogive followed by a fixed cross section mid and aft fuselage. The directional stability is provided by twin canted vertical tail placed on the aft fuselage. The control surfaces are elevons and rudders (ruddervators) used to trim the vehicle during longitudinal and lateral-directional motions. Reaction Control System (RCS) jets are used for three axis controls during the low dynamic pressure conditions.

RLV-TD ascent configuration is different from the conventional launch vehicles, where a wing body configuration on the top of solid booster produces large moment about the moment reference centre. The wing downwash influences the aft fin aerodynamic characteristic on the core base shroud. In the descent phase, during its reentry to touchdown, the RLV-TD flies at high to small angles of attack, covering high supersonic to low subsonic Mach numbers. The shear layer over the forebody and wing gets separated and rolls-up to form vortical flow at large angles of attack in the descent phase. The shock–vortex interaction results in very high unsteady levels. Due to the high angles of attack and resultant large separated flows, characterization of dynamic derivatives becomes important. The aerodynamic database generation is also quite huge, due to the large number of variables like Mach number, angle of attack, side-slip angle, elevon and rudder deflections. In comparison, a conventional launch vehicle has less number of variables for characterization and it is designed for a maximum of ± 4° angles of attack only. In a launch vehicle, the flow is attached to most of surfaces

Springer

except on the boattail or where-ever shock-boundary layer interaction takes place. Therefore, rigorous dynamic derivative characterization may not call for unlike in the wing body configuration. The basic aerodynamic characterization is also limited to small angles of attack at select critical Mach numbers.

Aeroacoustic is quite complex compared to aerodynamics. Steady state pressure distribution is sufficient for aerodynamics, whereas, unsteady pressure data is necessary for the aeroacoustic estimation. Wind tunnel test is the main source of generating unsteady pressure data using unsteady pressure models. Because, high fidelity CFD solvers like LES, DES are required to get the unsteady pressure data, but, the simulations are time consuming and requires high computing resources.

Fluctuating pressures during high Mach number regime are important design consideration due to their impact on the dynamic and strength characteristics of the vehicle structures [1]. Aeroacoustic levels are generated due to the unsteady pressure fluctuations of the flow over aerospace vehicle at high Reynolds number and during the lift-off due to the propulsive jet. Thus, the acoustic environment is created by rocket motors/engines and external aerodynamics. These acoustic loads may damage the payloads and launcher equipments [2]. Peak pressure fluctuations occur in the transonic flow conditions due to the transonic shock oscillation, shock induced flow separation and reattachment apart from the turbulent fluctuations in the boundary layer. The combination of the unsteady pressure fluctuation levels and the free stream dynamic pressure dictates the acoustic level. Therefore, it is possible that high dynamic pressure conditions may lead to higher acoustic levels than at transonic Mach numbers.

Other source of noise in launch vehicle is the due to the propulsive elements like rocket motors or engines, which generate high noise levels and it is felt by the complete vehicle during liftoff. Therefore, the characterization of aeroacoustics during liftoff is important. Aeroacoustics data due to rocket motors/engines are obtained from the static test of the scaled down motors (sub-scale test) or through empirical methods. There are three distinct components of noise are identified in a supersonic jet and they are (i) turbulent mixing noise, (ii) Mach wave radiation and (iii) broadband shock noise [3].

Aeroacoustic levels get transferred as structural vibration and may influence the structures, avionics packages performance and integrity of Thermal Protection System (TPS) tiles. High acoustic levels can cause higher vibration excitation on the structural, the propulsion elements like the valves, igniters, plumbing, avionics packages, etc. Low level excitation for a long period may cause structural failure due to fatigue. Therefore, the aeroacoustic

characterization and evolving the pre-flight envelop are important aspects for flight-worthiness of an aerospace vehicle.

Compared to launch vehicle aeroacoustic, the wing body configuration results in high acoustic levels due to vortex dominated flow, transonic shock-vortex interaction, likely vortex burst and the upstream influence of control surface deflections on the above flow phenomena. The adequacy of subscale wind tunnel tests for arriving at the vibro-acoustic design environments is demonstrated for the Space Shuttle ascent flight, where good correlations were observed with the wind tunnel acoustic data at lift off, transonic regime and maximum dynamic pressure conditions [4].

RLV-TD successfully demonstrated the autonomous hypersonic re-entry, controlled unpowered glided return flight and other technologies on 23rd May 2016. Post flight analysis of the pressure data and parameter estimations of force, moment coefficients and damping derivative compares well with the pre-flight data and are within the dispersions. In the present paper, the flight measured acoustic data is analysed and compared with pre-flight predictions.

Configuration

RLV-TD is a wing-body-twin vertical tail configuration as shown in Fig. 1. The wing is a double delta planform with 81° leading edge strake and 45° main wing sweep angles. The double delta planform reduces the centre of pressure travel and the small aspect ratio wing of 2.16 delays the stall. Reflex airfoil is used to improve the longitudinal stability and thereby, reduces the control surface deflection to trim the vehicle. The twin swept canted vertical tail with double wedge airfoil provides directional stability. Primary pitch and roll controls are through elevons placed at the trailing edges of the main wing and the yaw control is through rudders placed at the trailing edges of the twin
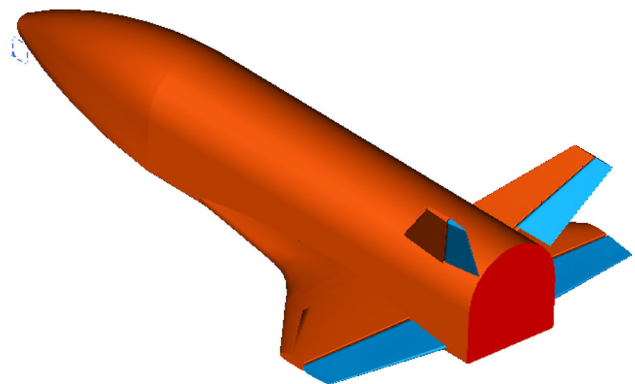

Fig. 1 RLV-TD descent configuration

canted vertical tail. The ascent configuration includes the RLV-TD placed at the top of HS9 solid booster. There are four fins placed in the core base shroud to improve the longitudinal stability. The root of portion of the fin is fixed on the core base shroud and tip portion is movable.

Five external microphones are mounted on the surface of RLV-TD at critical locations like on the leeward surface of fuselage-forebody, on the leeward side of the starboard wing, outboard surface of the starboard vertical tail, inter-stage (ITS), and Core Base Shroud (CBS). The microphone locations are schematically indicated on the ascent configuration in Fig. 2.

Pre-flight Acoustic Prediction Methodologies

Lift-Off Aero Acoustic Levels

Acoustic levels during lift-off due to the HS9 solid booster jet is predicted using spectrum source distribution (SSD) technique [5], where, the jet is divided into a number of
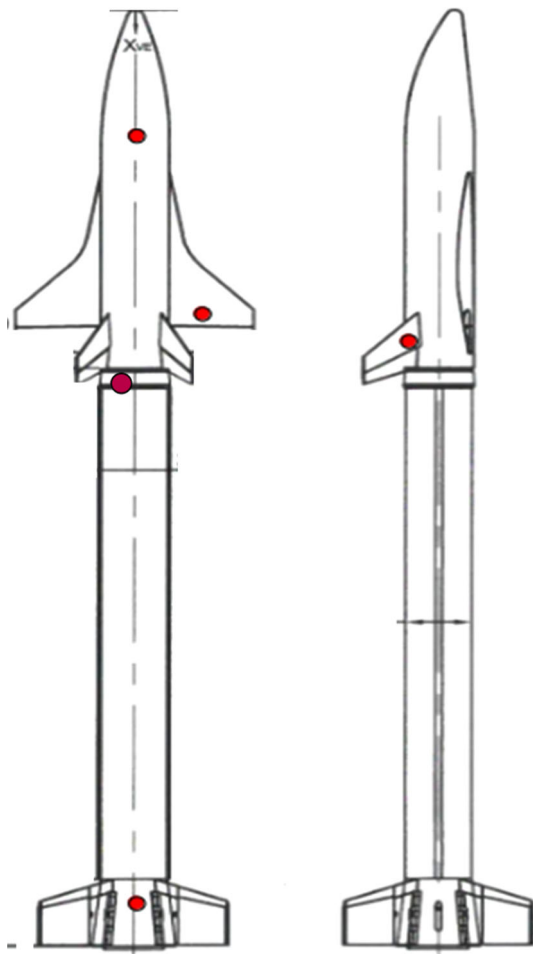

Fig. 2 Ascent configuration (microphone locations are shown)

slices with acoustic power is distributed in all frequencies. The acoustic power and its spectral distribution for each slice are calculated by using normalized relative source power spectra. The sound pressure level (SPL) at required location is estimated using the local directivity and inverse square law of sound propagation from all the slices. The jet noise is enveloped in the lift-off phase, that is, until the vehicle clears the umbilical tower. In the SSD method, the acoustic parameters are modeled based on the characteristics of free jet and distributed along the jet deflector. Therefore, the acoustic mechanism is not the same as that of free jet. Many studies have been carried out to improve the method described in NASA SP8072, nevertheless, the prediction accuracy so far demonstrated is insufficient because of the acoustic mechanism is not yet clearly understood and thus calls for sub-scale test [6].

In-Flight Aeroacoustic Levels

Pre-flight aeroacoustic levels are estimated using the unsteady pressure measurements over 1:10 scale unsteady pressure model of RLV-TD shown in Fig. 3 and few measurements from 1:15 scale aeroelastic model. The tunnel noise and the edge tone noise due to the transonic test section are removed from the power spectral density (PSD) data. The PSD data is scaled to flight conditions using the ratio of dynamic pressures, free stream velocities, and length scales based on boundary layer displacement thicknesses for regions where there is no separation. Geometric scaling is used where large scale flow separations are observed. The frequency is scaled using the Strouhal number.

The flight scaled wind tunnel PSD data is available only up to around 800 Hz and is extrapolated up to 8000 Hz to meet the flight conditions. The PSD data is first converted to 1/3rd octave band for each port and this data is enveloped across angle of attack and control surface deflections for each Mach number corresponding to the upper bound trajectory. Ascent trajectory envelopes are arrived at by using angle of attack $- 5°, 0°$ and $5°$ data. For the ITS levels, unsteady ports located in the aft region of fuselage were used. Unsteady pressure data from 1:15 scale aeroelastic model is used to arrive at the CBS levels. This data along with the lift-off jet acoustic levels are considered for arriving at the flight environmental test level (ETL) specification in the CBS region.

Flight Measured Acoustic Level Comparisons

The flight measured acoustic levels are obtained from five external microphones from lift-off to splash-down. Figure 4 shows the dynamic pressure and Mach number
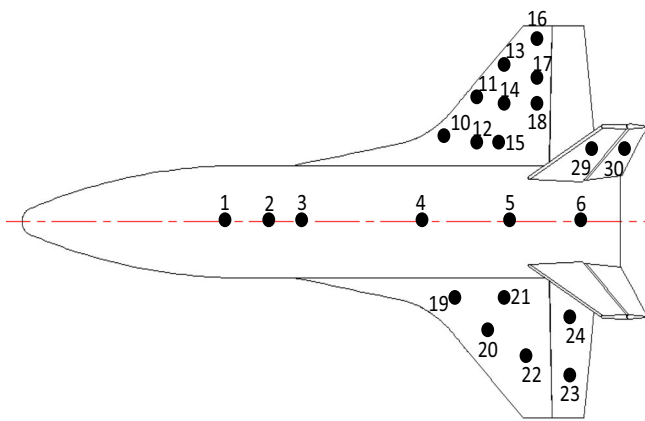
750

J. Inst. Eng. India Ser. C (December 2017) 98(6):747–755

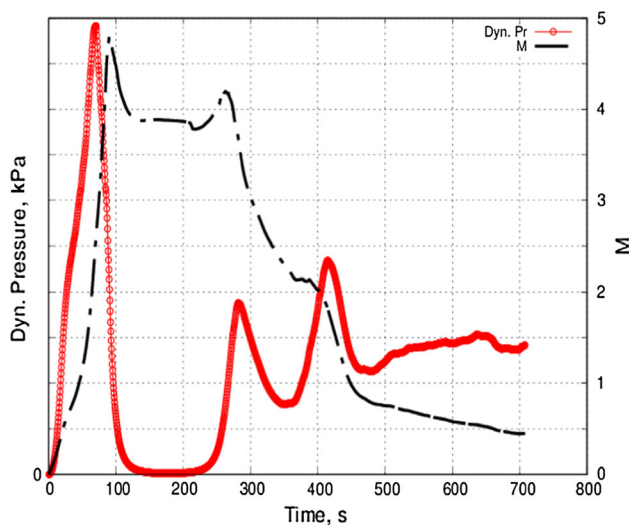**Fig. 3** Unsteady pressure model (1:10 scale) with pressure ports

Fig. 4 Dynamic pressure and Mach number variation along the flight trajectory

variation along the flight trajectory. The ascent mission is up to 180 s and thereafter, the descent mission starts. The measured unsteady pressure is processed on-board to get the SPL in 1/3rd octave band and transmitted back to the base stations.

Figure 5 shows the flight overall sound pressure levels (OASPL) variations on the fuselage forebody (FB), wing, vertical tail (VT), ITS and CBS from 0 to 770 s. The OASPL peaks at lift-off and during maximum dynamic pressure conditions in the ascent phase and during the transonic regime in the descent phase. The highest acoustic level occurs on CBS and wing in the ascent and descent phases respectively.

Figure 6 shows the OASPL comparison with pre-flight prediction during lift-off. The flight data compares well with pre-flight prediction based on SSD method at different lift-off instances of 0 s (0 m), 1.41 s (5 m), 1.95 s (10 m) and 2.37 s (15 m). During the lift-off, high acoustic

levels are observed due to HS9 solid booster jet. As expected, the maximum level occurs on CBS due to its proximity to the jet. The corresponding pre-flight estimate using SSD technique is lower by 2.8 dB. When the vehicle is at 5, 10 and 15 m from the pedestal, the prediction is higher by a maximum of 2.9 dB. Acoustic levels at ITS, vertical tail, wing and forebody decreases with inverse-square of the distance from the jet. For fuselage forebody, wing, vertical tail and ITS the trend of OASPL and magnitude are similar (within a maximum of 1.8 dB at t = 2.37 s) and the comparison with the pre-flight prediction is good. The reason for the large dip (between 0.5 and 1.5 s) in the acoustic levels for the ITS and CBS is not known and needs further investigation. Overall, the pre-flight prediction during lift-off matches reasonably well with the flight data.

Figure 7 shows the flight measured acoustic levels during the ascent phase. The figure also shows the OASPL predictions for the flight trajectory processed in the frequency range of 31.5–3150 Hz corresponding to the flight range. It is seen that after the transonic shock passes over the microphone, there is a distinct fall in the acoustic level. The transonic shock occurs on the wing at lower transonic Mach number (t = 38.5 s, M = 0.77) compared to the forebody, vertical tail and ITS, where, the shock occurs slightly later (t = 42.5 s, M = 0.93). For CBS, the transonic shock signature is seen at t = 40 s.

Due to rapid expansion over the wing, the transonic shock formation takes place at lower free stream Mach number. On the other hand, the ogive forebody delays the transonic shock formation over the fuselage to a higher transonic Mach number and also reduces the shock strength. The maximum OASPL occur at transonic conditions below M = 1 for wing, fuselage and vertical tail. For the ITS, the maximum level occurs at t = 49 s, at M = 1.12. Overall maximum acoustic level occurs for CBS from t = 67 s to 70 s, (M = 2.27 to 2.58) due to

Fig. 5 Flight OASPL variation
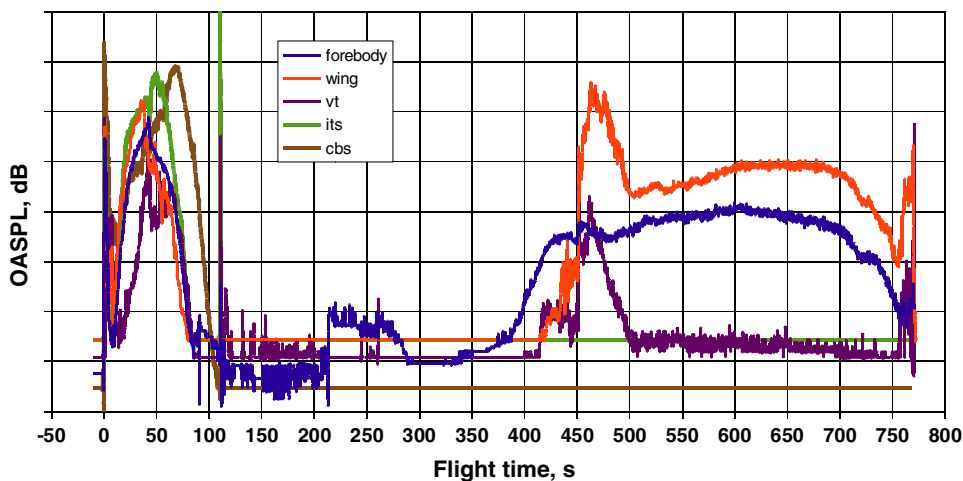in the ascent and descent phases

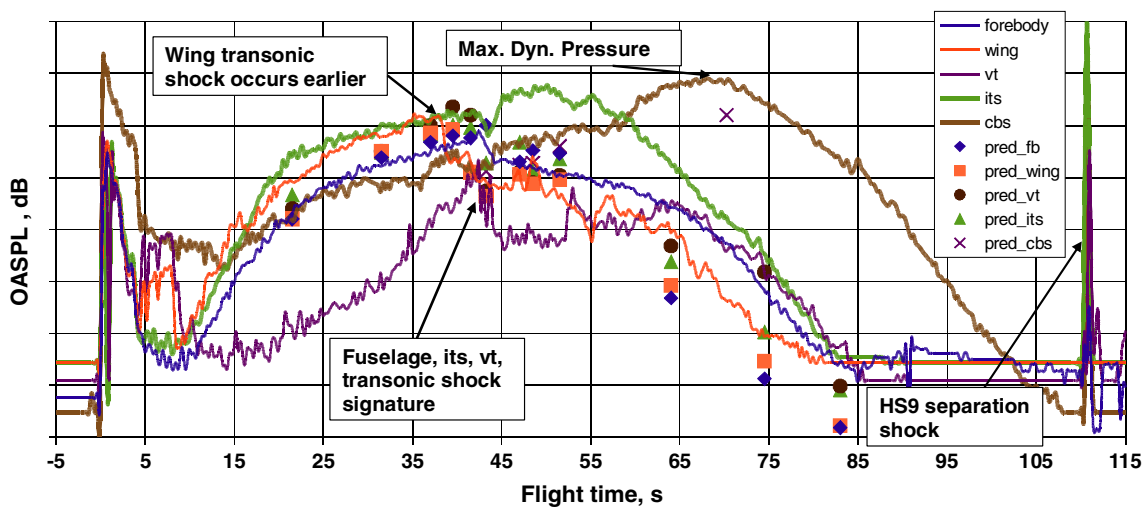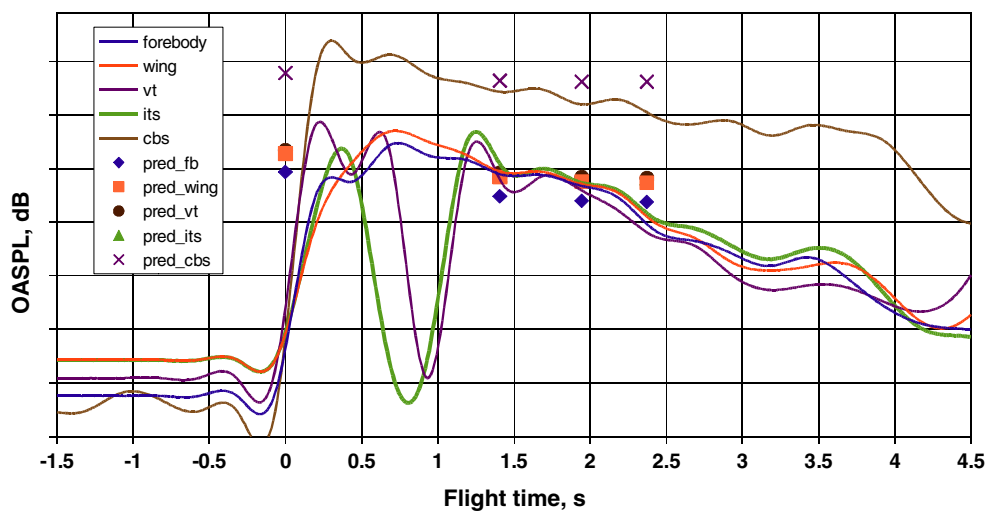**Fig. 6** Flight OASPL
comparison with prediction
during lift-off

Fig. 7 Flight OASPL comparison with prediction in the ascent phase

752

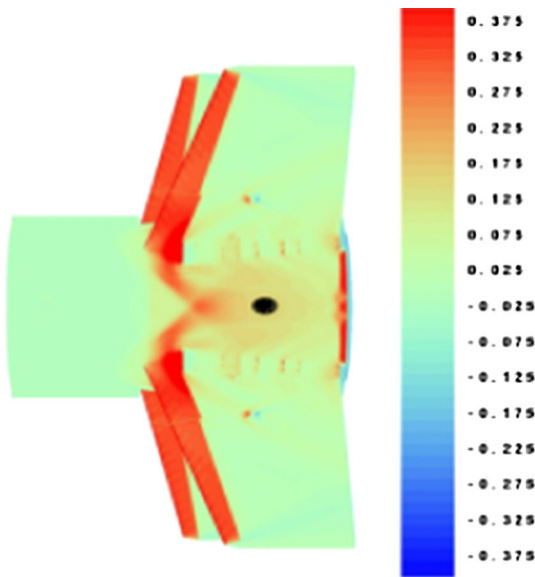J. Inst. Eng. India Ser. C (December 2017) 98(6):747–755

Fig. 8 Shock-shock interaction at M = 2.5 due to booster fins

(i) maximum dynamic pressure condition (t = 70 s) and (ii) the proximity of the shock-shock interference. These shocks originate from the booster fins as shown in Fig. 8, (figure also indicate the microphone location). The CBS prediction is 2.1 dB lower compared to the peak flight value. It is seen that the peak level predictions for VT is higher by 4.5 dB, on ITS it is lesser by 4.8 dB and for fuselage and wing it is within 2.1 dB.

Figure 9 shows the flight OASPL with predictions for wing, fuselage and vertical tail during the descent phase from t = 380 s to 580 s. The transonic shock signature is seen at t = 450 s (M = 0.977) for fuselage, t = 450.94 s (M = 0.966) for the wing and t = 451.68 s (M = 0.956) for the vertical tail. The occurrence of transonic shock

signature is seen nearly at the same time for fuselage, wing and VT. Apart from the transonic shock signature at t = 450 s, there are sudden changes seen at the peak value for the wing at t = 461.937 s (M = 0.866) and vertical tail at t = 461.43 s (M = 0.868).

Highest OASPL level occurs over the wing and the prediction is under predicted by 6 dB at transonic Mach numbers. This deviation in the predicted level is attributed to; (i) non-availability of exact unsteady pressure port location in the pre-flight wind tunnel test, (ii) non-availability of exact flight angle of attack and control surface deflections from the unsteady database, and (iii) clean surface finish on the unsteady model compared to the flight configuration, where, TPS tiles and flexible blankets are applied. The predictions for the fuselage forebody (within 1 dB) and vertical tail (within 1.8 dB) are good. The vertical tail OASPL values falls and remain constant at a lower value from 500 s is not as expected.

Figure 10 shows the Mach palettes at M = 0.95 and 0.9 for the fuselage and wing obtained through CFD simulations using PARAS-3D. Small sonic pockets are terminated by a transonic shocks on the fuselage forebody are due to the undulations of thermal flexible insulation. Transonic shock is also seen on the wing top and bottom surfaces. These shock signatures nearly corresponds to the transonic OASPL levels observed in Fig. 9 over fuselage, and wing.

RCS Signature in the Measured Acoustic Levels

Reaction control system (RCS) jets are fired during the low dynamic pressure conditions during ascent and descent phases to control the vehicle. During lift-off, the roll RCS on the wings are fired for the roll control. Figure 11 shows
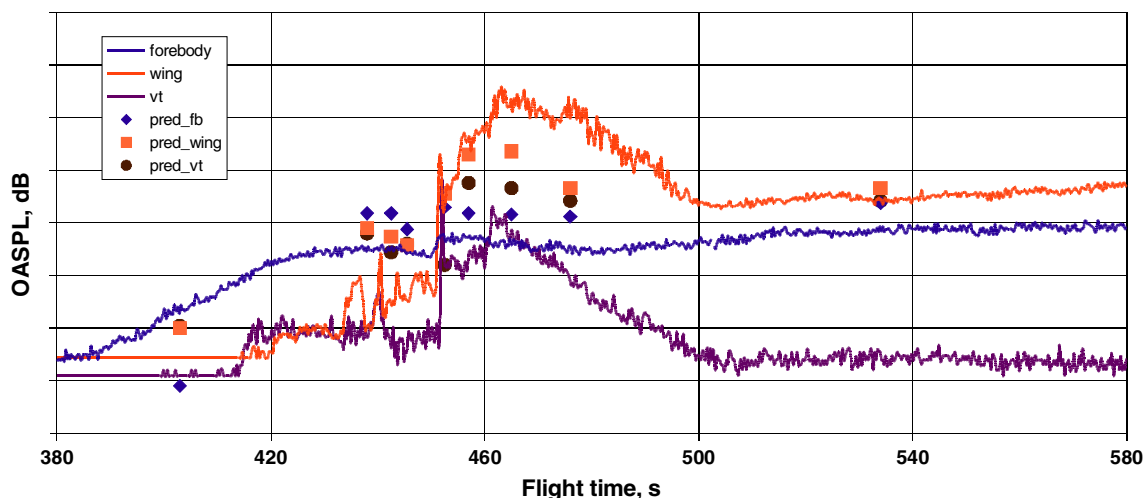

Fig. 9 Flight OASPL comparison with prediction in the descent phase

Fig. 10 Mach palette over fuselage and wing with flow expansion region at M = 0.95 and 0.9

T=453s, M=0.95

T=453s, M=0.95
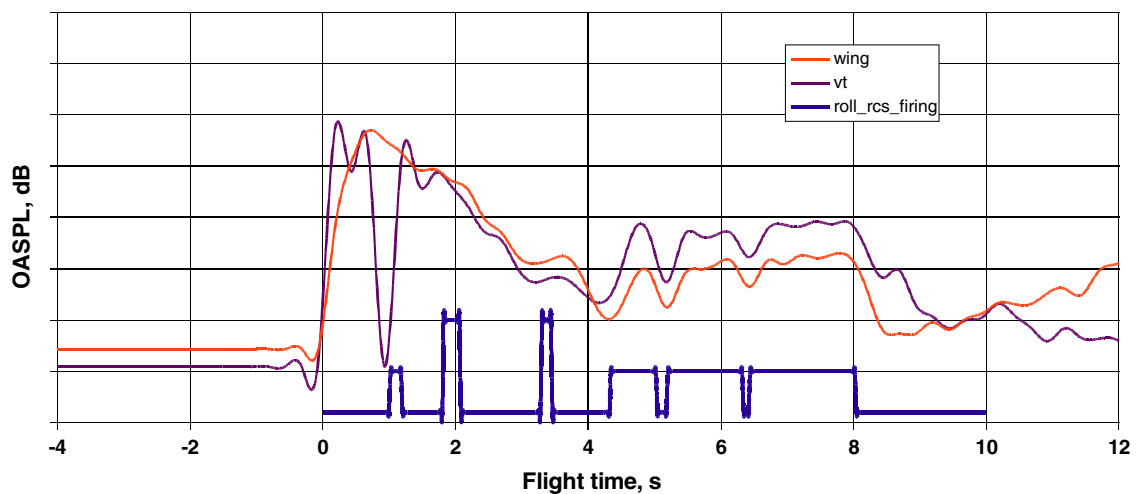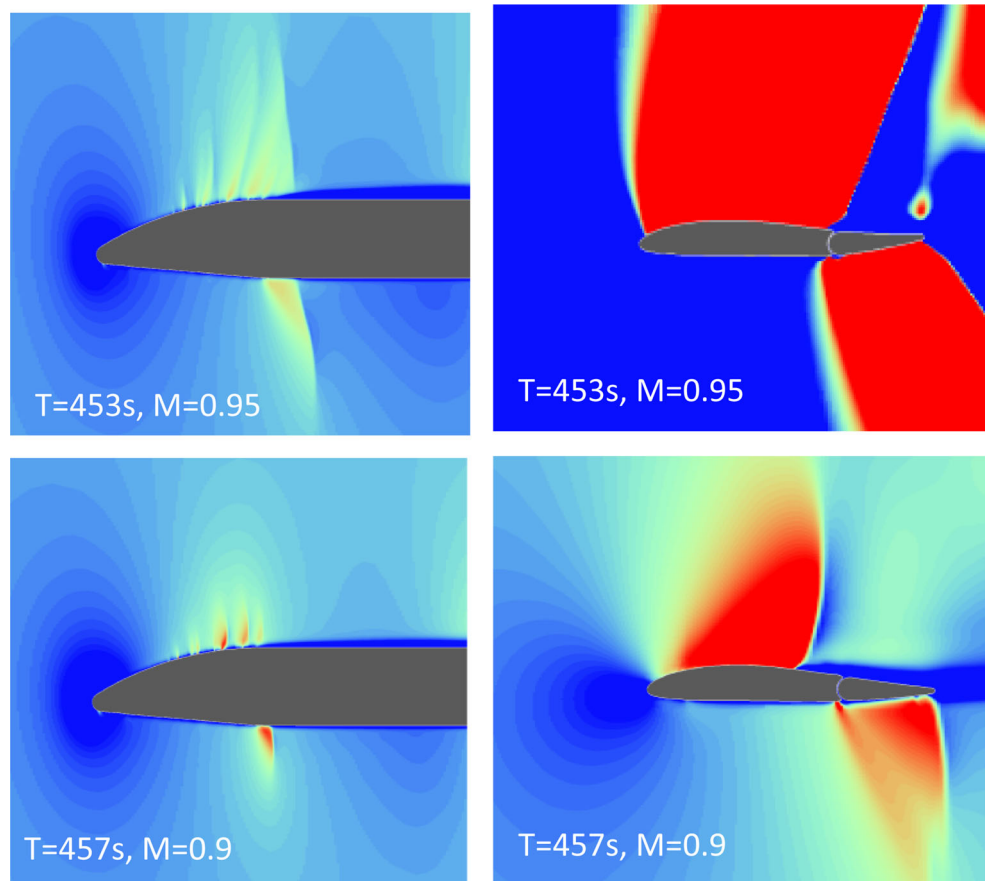
T=457s, M=0.9

T=457s, M=0.9

Fig. 11 Flight OASPL levels during lift-off show the roll RCS firing signature on the wing and vertical tail

the flight acoustic levels during lift-off up to 15 s on the wing and vertical tail. The insert in the Fig. 11 shows the roll RCS firing from 1 to 8 s, the tall signals corresponds to roll to left and short signals corresponds to roll to right. Up to 4 s the booster motor acoustic level influences the acoustic levels at all the locations. A series of roll to right signals are seen from t = ~ 4 to 8 s and the OASPL also shows the peak and fall corresponding to the roll RCS firing during the lift off in the ascent phase. The effect of roll RCS firing increases the OASPL by 5–7.5 dB and higher levels are observed on the VT compared to the wing.
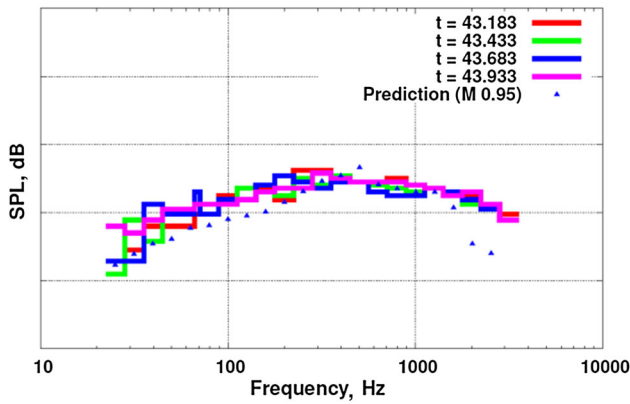
754

J. Inst. Eng. India Ser. C (December 2017) 98(6):747–755
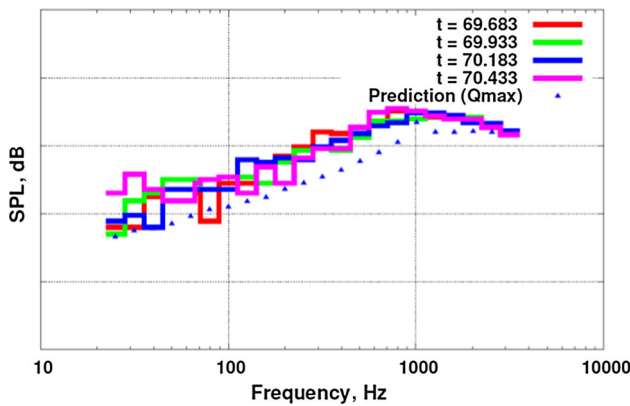

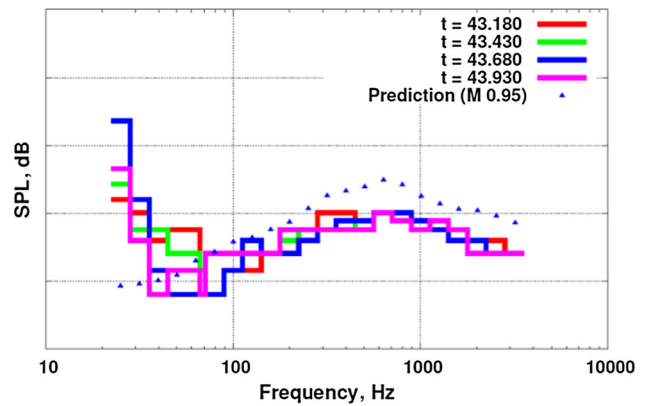
Fig. 12 CBS spectrum at M = 0.95 during ascent phase

Fig. 13 CBS spectrum at M = 2.6 during ascent phase

Spectrum Comparison

Figures 12 and 13 show the SPL spectra comparison of the CBS at Mach number ∼ 0.95 and ∼ 2.6, respectively. The spectra are plotted at 4 time instants. The spectrum comparison at M = 0.95 compares well with the prediction except at the high frequency. The spectrum comparison at maximum dynamic pressure condition at M = 2.6, indicate

Fig. 15 Wing spectrum at M = 0.77 during ascent phase

Fig. 16 Vertical tail spectrum at M = 0.95 during ascent phase

slight under prediction compared to flight. At M = 2.6, the trend is different compared to M = 0.95. Figure 14 shows the fuselage SPL comparison at M = 0.93. The prediction is higher compared to the flight spectrum and there is a cross over at 1000 Hz due to the faster decay of the SPL from the unsteady wind tunnel database. Figure 15 shows the wing SPL comparison at M = 0.77. The prediction compares well with the flight measurements up to 700 Hz
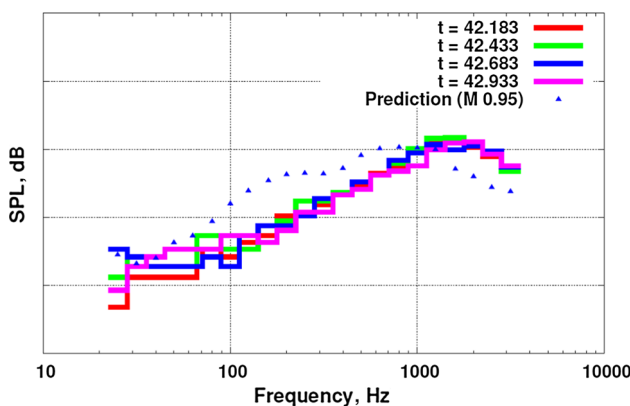

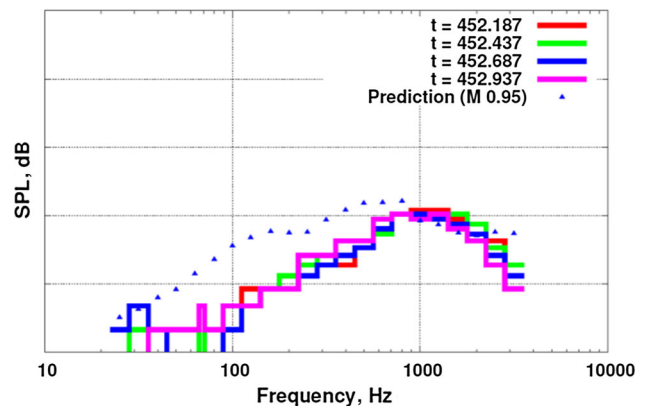**Fig. 14** Forebody spectrum at M = 0.93 during ascent

Fig. 17 Forebody spectrum at M = 0.95 during descent phase

J. Inst. Eng. India Ser. C (December 2017) 98(6):747–755
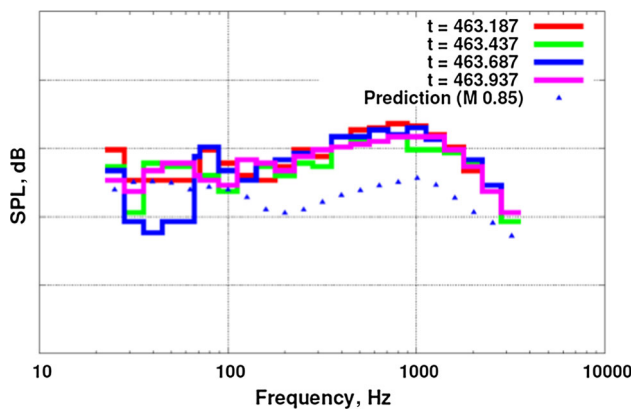
755

Fig. 18 Wing spectrum at M = 0.86 during descent phase

above this frequency the decay of the SPL is faster. Vertical tail spectrum comparison is shown in Fig. 16 at M = 0.95. The prediction is slightly higher compared to the flight spectrum but the trends are captured.

Figure 17 shows the fuselage descent spectrum at M = 0.95, the prediction is higher up to 1000 Hz and above this frequency the match is good. Figure 18 shows the wing spectrum at M = 0.86, where the prediction is good up to 100 Hz and above this frequency the spectrum is under-predicted.

Conclusions

RLV-TD was successfully flight tested on 23rd May 2016. There were five microphones located on the external surfaces to measure the in-flight acoustic levels from lift-off to splash-down. The measured lift-off noise levels are higher than the prediction by a maximum of 2.8 dB. Measured levels on core base shroud recorded the overall maximum at both lift-off and transonic conditions during ascent phase. In-flight noise levels measured in ascent phase on the wing is second highest, followed by fuselage and vertical tail. Predictions for flight trajectory during ascent phase compare well at all locations except for vertical tail (4.5 dB). Maximum measured OASPL during descent transonic regime occurs on the wing, followed by vertical tail and fuselage. Predictions for flight trajectory during descent phase compare well at all locations except for wing (− 6.0 dB).

Overall, spectrum comparison is good for CBS, wing and vertical tail at maximum OASPL conditions and deviations at peak OASPL is seen for the fuselage in the ascent phase. In descent phase, under and over predictions are seen at peak condition for wing and fuselage respectively. The vertical tail trend is not as expected. The roll RCS thruster firing signature is seen in the acoustic measurements on the wing and vertical tail during the initial lift-off time period.

References

1. A.L. Laganelli, H.F. Wolfe, Prediction of fluctuating pressure in attached and separated turbulent boundary-layer flow. J. Aircr. **30**(6), 962–970 (1993)
2. N.S. Dougherty, S.H. Guest, A correlation of scale model and flight aeroacoustic data for the space shuttle vehicle. In *AIAA-84-2351, AIAA/NASA 9th Aeroacoustics Conference*, 15–17 Oct 1984, Williamsburg, Virginia
3. K.M. Eldred, *Acoustic loads generated by the propulsion system*. NASA SP-8072 (1971)
4. B. Troclet, S. Vanpeperstraete, M.-O. Schott, Experimental analysis of lift-off and aerodynamic noise on the Ariane 5 Launch Vehicle. In *CEAS/AIAA-95-070*, p. 535–544 (1995)
5. M. Kandula, Prediction of turbulent jet mixing noise reduction by water injection. AIAA J. **46**(11), 2714–2722 (2008)
6. S. Tsutsumi, T. Ishii, K.Ui, S. Tokudome, K. Wada, Study on acoustic prediction and reduction of epsilon launch vehicle at liftoff. J. Spacecr. Rockets **52**(2), 350–361 (2015)